

# Experimental validation of a tactile sensor model for a robotic hand

S. Yahud, S. Dokos, J.W. Morley and N.H. Lovell, *Senior Member, IEEE*

**Abstract**— We describe a tactile sensor for a robotic hand, based on the mechanoreceptors in the glabrous skin of the human hand to replicate the sensory function of both slow adapting and fast adapting receptors. Strain gauges are used for the slow adapting receptors, and polyvinylidene fluoride (PVDF) film was used to replicate the function of the fast adapting receptors. One unit sensor consisted of four strain gauges and a single PVDF film, embedded beneath a square protrusion. The protrusion helped localize the applied force onto the region or ‘receptive field’ of the sensing unit. Strain gauges were orientated to enable the unit sensor to identify the tri-axial force components. Multiple linear regression was used to predict the components of force. The regression model with interaction terms gave good prediction with mean percentage errors of less than 15% for each force component.

## I. INTRODUCTION

Tactile sensors serve an important role in robotic and prosthetic applications. An important requirement in robotic hand tactile sensor design is the ability to sense normal and shear components of force, as well as high-frequency vibrations which may arise during slippage of objects that are gripped. Our design of such sensors is inspired by the function of the mechanoreceptors in the glabrous skin of the human hand, whereby receptors are classified into two groups, –fast adapting and slow adapting, based on their adaptation to “ramp and hold” tactile stimuli. Fast adapting receptors primarily respond to contact onset and offset, whereas slow adapting receptors respond to initial contact and maintain neural firing throughout the contact period [1].

Strain gauges are used to emulate the function of both Merkel cells and Ruffini endings, both slowly adapting receptors, whereas polyvinylidene fluoride (PVDF) film was introduced to emulate Pacinian corpuscles that are fast adapting receptors. Changes in effective gauge length of resistive elements in the strain gauge are a measure of the static force applied. In contrast, PVDF is a piezoelectric material which generates electrostatic charge due to applied mechanical stress [3]. The higher the applied frequency, the more electric current is required to produce the same stress-induced charge density per unit time. Thus, PVDF is able to respond to rapidly varying mechanical stresses, similar to fast adapting mechanoreceptors [4-5].

S. Yahud is with the Graduate School of Biomedical Engineering, University of New South Wales, NSW, Australia, and is pursuing her PhD under sponsorship of the School of Mechatronic Engineering, University of Malaysia Perlis.

S.Dokos and N.H. Lovell are with Graduate School of Biomedical Engineering, University of New South Wales, NSW, Australia

J.W. Morley is with School of Medicine, University of Western Sydney, Penrith, Australia

The authors would like to thank Philip Byrnes–Preston for expert assistance in the electronics design. This project is funded by an Australian Research Council (ARC) Thinking Systems grant.

The texture of the glabrous skin also plays an important role during object handling. A square protrusion was introduced in the design as an attempt to emulate epidermal ridges of the finger tips to provide friction and better grip [6-9]. This concept is employed in the present design to enable the sensor to detect tri-axial force components as well as vibration.

A finite element model was used in the preliminary stage of this study to investigate the behavior and performance of the proposed unit sensor [10]. Rudimentary experimental validation was also performed to confirm the predicted output obtained from the finite element analysis (FEA). Multiple linear regression was carried out to predict the applied components of force from the strain gauge signals. This study aims to validate the initial findings from our FEA of strain gauge outputs and our regression approach used to identify the components of force.

## II. SENSOR STRUCTURE

### A. Theory

The proposed unit sensor consists of four strain gauges and one PVDF film embedded in a silicone elastomer. These five sensing elements are located beneath a square protrusion of  $2 \times 2 \text{ mm}^2$ . Fig. 1 shows the configuration of our unit tactile sensor (a  $12 \text{ mm} \times 12 \text{ mm}$  block, with  $3 \text{ mm}$  thickness and  $4 \text{ mm}^2$  square protrusion of  $1 \text{ mm}$  height located on the middle top surface). These dimensions were chosen to house four commercial strain gauges (632-124, RS Components, Japan) of  $2 \text{ mm}$  effective gauge length. The strain gauges were arranged in an orientation which allowed the unit sensor to detect forces in orthogonal directions,  $F_x$ ,  $F_y$ , and  $F_z$  accordingly.

From the considerations of symmetry, we expect the components of forces to be determined as follows:

$$F_x = \alpha(S_3 - S_1) \quad (1)$$

$$F_y = \alpha(S_2 - S_4) \quad (2)$$

$$F_z = \beta(S_1 + S_2 + S_3 + S_4) \quad (3)$$

where  $S_1, S_2, S_3, S_4$  are the strain gauge signals and  $\alpha, \beta$  are proportionality constants. The PVDF film was placed below the protrusion,  $1 \text{ mm}$  directly beneath the four strain gauges, similar to the position of Pacinian Corpuscles in the glabrous skin [1-2]. The protrusion was added to help localize pressure from the applied load onto the “receptive field” of the sensing area. The limitation of this approach is that the contact area between a handled object and the sensor will be limited to the protrusion surface. The advantages however, is that it simplifies the problem of force detection to a known location. The unique deformation of the protrusion under

various loading conditions facilitates the identification of the contributing components of the applied force.

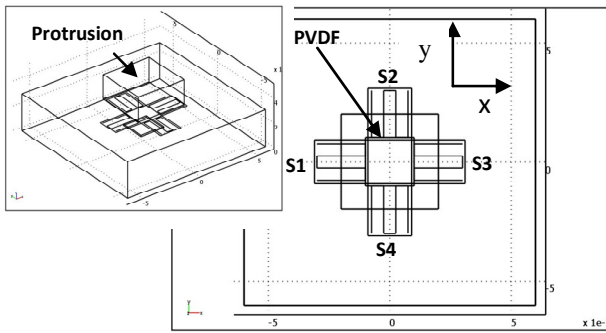


Fig.1. The proposed unit sensor consists of four strain gauges ( $S_1 - S_4$ ) and one PVDF film embedded in a silicone elastomer block.

### B. Finite Element Analysis

An FEA study was conducted under the assumptions that the silicone elastomer was a homogenous, nearly incompressible, and isotropic hyperelastic medium, using Comsol Multiphysic software (Comsol, AB). Strain gauges were modeled as an edge element within a polyimide thin shell. Simulated elongation of strain gauge edge elements was calculated and used as strain gauge signals ( $S_1 - S_4$ ), to develop multiple linear regression models to predict the applied components of force. The PVDF film was modeled as a piezoelectric material using the strain-charge constitutive form. FEA confirmed that the protrusion helped to transmit force onto the sensing elements. All four strain gauges were deformed in a similar way under uniform normal load. Shear force on the protrusion resulted in tension on one side and compression on the other side, as sensed by opposing strain gauges. The difference between these two gauges corresponded to shear force applied on the protrusion. Stimulated strain gauge outputs were successfully able to identify the tri-axial forces experienced by the proposed unit sensor [10].

### C. Experimental setup

The unit sensor was composed of four strain gauges of 2 mm effective gauge length, (632-124, RS Components, Japan),  $2 \times 2 \text{ mm}^2$  PVDF film (Special Measurement, USA), embedded in silicone elastomer (Sylgard 184, Dow Corning, UK). The four strain gauges and the PVDF film were carefully aligned in the orientation proposed. Silicone was poured into a mould and cured at room temperature. A constant current loop and a voltmeter circuit measuring electrical potential difference between strain gauge voltage and reference voltage was used to assess the change in resistance experienced by the gauge. The PVDF output will not be discussed further in this study, but the PVDF film was embedded underneath the four gauges to retain the structure of the proposed unit sensor as solved in the FEA model.

The experimental setup consisted of a loading structure, a signal conditioning unit, data acquisition system and data

analysis software. As shown in Fig. 2, forces were applied on the sensor by moving a force gauge in the Z-direction and contacting the protrusion using a probe with an angled tip (diameter  $\approx 4 \text{ mm}$ ). The probe was custom-made for each tilt angle, to ensure a complete contact with the surface of the protrusion. The digital force gauge was mounted on a micromanipulator, (DC3, Märzhäuser Wetzlar) and controlled using a micromanipulator controller, (MS314, Märzhäuser Wetzlar) at a constant speed of  $0.2 \text{ mm/s}$ . The analogue output of the force gauge (Advanced Force Gauge (AFG), Mecmesin) was calibrated to give the measured output in unit force, N.

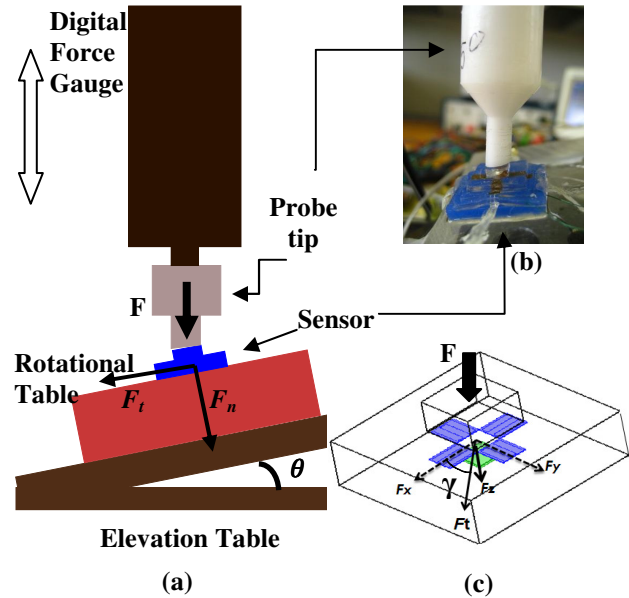


Fig.2. (a) Experimental setup for force application in X, Y and Z directions simultaneously. Compression load is measured using a digital force gauge. (b) Flat angle probe to ensure a complete contact with the surface of the protrusion. (c) Definition of rotation and elevation angles ( $\theta, \gamma$ ) of compression load on unit sensor.

Components of force could be determined from the tilt ( $\theta$ ) and rotation ( $\gamma$ ) angle of elevation and rotational table accordingly. An elevation table was used to elevate the rotational table to angle  $\theta$ , giving force components in the normal and horizontal direction as given in (4) and (6). A rotational table was used to rotate the sensor in the XY plane, by an angle  $\gamma$ , such that in the reference configuration  $S_3$  will be on  $\gamma = 0^\circ$ . The force in the transverse direction,  $F_t$  is further resolved, giving  $F_x$  and  $F_y$  in (7) and (8).

$$F_z = F \cos \theta \quad (4)$$

$$F_t = F \sin \theta \quad (5)$$

$$F_x = F_t \cos \gamma \quad (6)$$

$$F_y = F_t \sin \gamma \quad (7)$$

Strain gauges signals and applied force data were sampled at a 3 kHz rate through a 14-bit NI USB-6009 data acquisition system and a LabVIEW 8.2 (National Instruments, USA) program.

A multiple linear regression method was used to predict each component of force from the output signals of the strain gauges. Interaction terms were added to incorporate the joint effect of all four gauges. The multiple linear regression model used to predict the force components is given in (8).  $\beta_{0-14}$  are the 15 regression coefficients corresponding to signals  $S_1, S_2, S_3,$  and  $S_4$  including interaction and quadratic forms.

$$\begin{aligned} \hat{F}_{x,y,z} = & \beta_{0x} + \beta_{1x}S_1 + \beta_{2x}S_2 + \beta_{3x}S_3 + \beta_{4x}S_4 + \beta_5S_1S_2 \\ & + \beta_6S_1S_3 + \beta_7S_1S_4 + \beta_8S_2S_3 + \beta_9S_2S_4 + \beta_{10}S_3S_4 \\ & + \beta_{11}S_1^2 + \beta_{12}S_2^2 + \beta_{13}S_3^2 + \beta_{14}S_4^2 \end{aligned} \quad (8)$$

### III. RESULTS AND DISCUSSION

The ability of the sensor to identify both normal and shear forces was investigated. Force applied on the protrusion was varied from 0 to 5 N at elevation angles of  $0^\circ, 5^\circ, 10^\circ,$  and  $20^\circ$ . At each elevation angle, the sensor was rotated from  $0^\circ$  to  $360^\circ$  in increments of  $15^\circ$ . Strain gauge outputs were tested for normal loads ( $\theta=0^\circ$ ), to confirm all four gauges were responding linearly under compression.

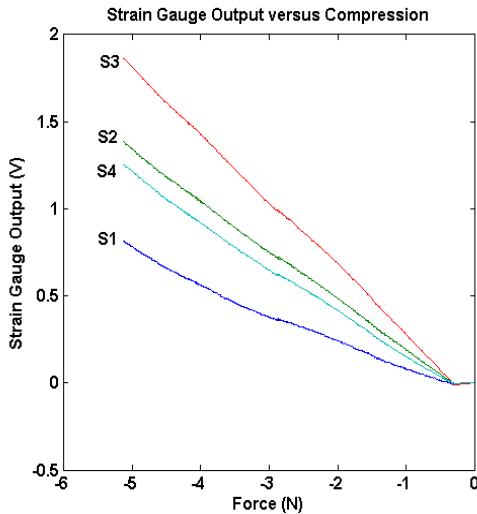


Fig.3. Strain gauge outputs as a function of normal compression load.

Strain gauge outputs were varied approximately linearly with normal compression, as illustrated in Fig. 3. The result presented confirmed the FEA result that strain gauge outputs are linear with applied load. Different output slopes indicate that the strain gauges have different sensitivities to applied force. This is most likely due to variations in strain gauge placement during the fabrication process.

Statistical details of the multiple regression performed on each component of force based on strain gauge outputs are summarized in Table 1. The high  $F$ -stat value and  $p$ -value lower than 0.05 suggest that the regression model (8)

provides a good fit to the data. Fig. 4 illustrates the predicted  $F_x$  and  $F_z$  components for all experiments conducted against actual loads.

TABLE 1  
IN SUMMARY OF MULTIPLE REGRESSION MODEL FOR EACH DIRECTION OF FORCE

Component of forces	$R^2$	$F$ -Stat	$p$ -value	Estimate of the error variance
$F_x$	0.9100	292.3958	<0.01	0.0307
$F_y$	0.8395	151.2948	<0.01	0.0513
$F_z$	0.9753	1142.4	<0.01	0.0766

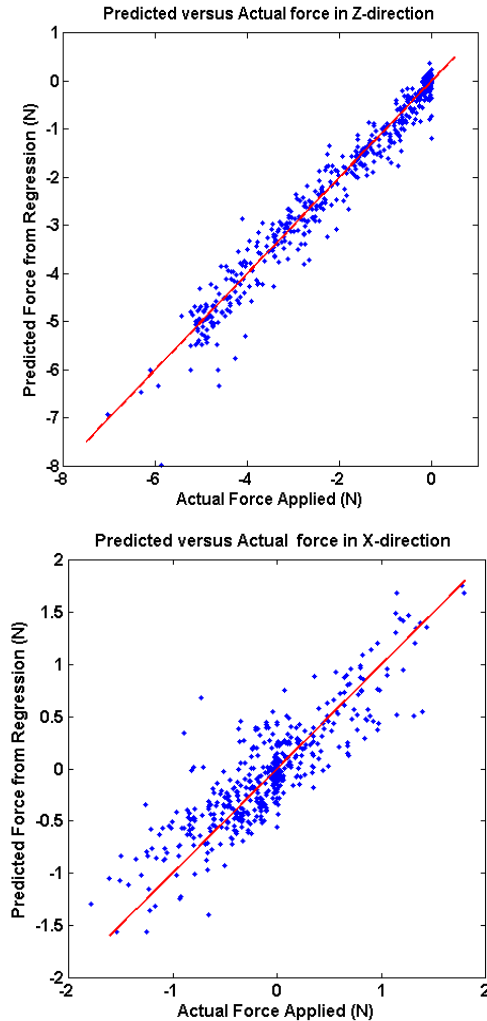


Fig.4. Regression output for  $F_x$  and  $F_z$  shows that the predicted component of force corresponds with the known applied force. The solid line is the ideal  $F_{predicted} = F_{applied}$ .

The accuracy of the regression model was further examined by applying the strain gauge signals to (8), and comparing the predicted force components against known applied forces. Fig. 5 shows the predicted  $F_x$  and  $F_z$  against the actual components of force applied on the sensor for a particular elevation angle,  $\theta = 20^\circ$  and rotated,  $\gamma = 120^\circ$  from  $S_3$ .

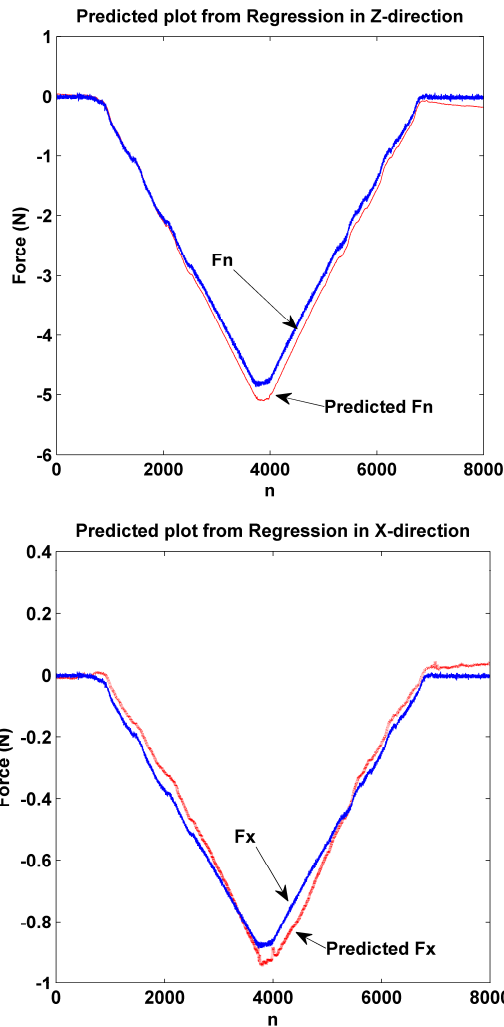


Fig.5. Predicted force for each component and calculated components,  $F_x$  and  $F_n$ , at  $\theta = 20^\circ$ , and  $\gamma = 120^\circ$

Considering the configuration of the strain gauges and the function of the protrusion in the sensor, shear components determined in either X or Y directions will be equal in magnitude for opposite direction of applied load provided the strain gauges have the same sensitivity. Therefore in this paper, only one direction of predicted shear will be presented.

TABLE 2  
MEAN ERROR FOR PREDICTED FORCE AT  $\theta=20^\circ, \gamma=120^\circ$

	Mean Error (%)
$F_x$	3.93
$F_y$	14.22
$F_n$	13.16

Mean errors for the predicted tri-axial components of force at ( $\theta = 20^\circ, \gamma = 120^\circ$ ) are shown in Table 2. These results show that the multiple linear regression model is providing reasonable predictions of applied forces, for tri-axial components with mean errors less than 15%. The difference between our unit sensor compared to previous

approaches [5-7] is the multiple linear regression model which is robust enough to predict tri-axial forces even with substantial variation in gauge sensitivity.

#### IV. CONCLUSION AND FUTURE WORK

Our unit sensor was able to differentiate the tri-axial force components based on the strain gauge outputs. Experimental results verify the FEA model in the early stages of the study. In future work, output from the PVDF will be incorporated with the strain gauge outputs to produce an algorithm to detect slip. In the future a microelectromechanical (MEMS) fabrication technique will be explored to custom-make strain gauges with the aim of eliminating error in positioning as well as reducing both the protrusion area and the overall sensor size.

#### REFERENCES

- [1] L. A. Jones, S. J. Lederman, *Human Hand Function*, Oxford University Press, Inc., New York, 2006, pp. 24-43.
- [2] T. Maeno, K. Kobayashi, N. Yamazaki, "Relationship between the structure of human finger tissue and the location of tactile receptors", *Jsmc International Journal Series C-Mechanical Systems Machine Elements and Manufacturing*, vol. 41, pp. 94-100, 1998.
- [3] *Piezo film sensors technical manual*, Measurement Specialties, Inc., Rev D, 15 March 2006.
- [4] L. Weiting, A. Menciassi, S. Scapellato, P. Dario, Y. Chen, "PVDF-based biomimetic sensor for application in crawling soft-body mini-robots", *IEEE/RSJ International Conference on Intelligent Robotic and Systems*, pp. 1960-1965, 2006.
- [5] M.A. Qasaimeh, S. Sokhanvar, J. Dargahi, M. Kahrizi, "PVDF-based microfabricated tactile sensor for minimally invasive surgery", *Journal of Microelectromechanical Systems*, vol. 18, pp. 195-207, 2009.
- [6] I. Fujimoto, Y. Yamada, T. Morizono, Y. Umetani, T. Maeno, "Development of artificial finger skin to detect incipient slip for realization of static friction sensation", *IEEE Conference on Multisensor Fusion and Integration for Intelligence System*, pp.15-20, 2003.
- [7] E-S. Hwang, J-H. Seo., Y-J. Kim, "A polymer-based flexible tactile sensor for both normal and shear load detections and its application for robotics", *Journal of Microelectromechanical Systems*, vol.16, pp. 556-563, 2007.
- [8] J. Engel, J. Chen, C. Liu, "Development of polyimide flexible tactile sensor skin", *Journal of Micromechanics and Microengineering*, pp. 359, 2003.
- [9] J-H. Kim, J-I. Lee, H-J. Lee, Y-K. Park, M-S. Kim, D-I. Kang, "Design of flexible tactile sensor based on three component force and its fabrication", *IEEE International Conference on Robotics and Automation*, pp. 2578-2581, 2005.
- [10] S. Yahud, S. Dokos, J.W. Morley, N.H. Lovell, "Finite element analysis of a tactile sensor for a robotic hand", *ISSNIP International Conference on Intelligent Sensors, Sensor Network and Information Processing*, ISSNIP 2008, pp. 335-340, 2008.